

DETERMINING OF NEUTRAL AND UNSTABLE WIND PROFILES OVER BAGHDAD CITY

Monim H. Al-Jiboori

Department of Atmospheric Sciences, College of Sciences, University of Al Mustansiriya, Baghdad-Iraq.

Abstract

This paper provides a comprehensive analysis of slow-response observations taken over the centre of Baghdad city (Bab Al-Mhadham area). Measurements were taken at two levels: 15 and 20 m and then wind speed profiles were derived according to atmospheric stability indicated by Richardson number in the lower part of planetary boundary layer. These profiles were constructed by logarithmic and power-exponent laws after checking estimated winds at the same heights by these laws with those observed. The estimated values of wind at these levels were in good agreement with observed values. Mean wind profiles calculated from both laws have logarithmic behavior especially in neutral conditions. They have the same shape and values at lower heights up to 50 m and then gradually deviate from each other over this height. Lastly, drag coefficient at each level was calculated and then its results found to be constant over neutral regime and increased with increasing instability.

1. Introduction

Knowledge of the mean wind speed in the surface layer, the lowest 10% of the planetary boundary layer (PBL), is of special importance for air pollution, wind energy and other

applications. Unfortunately, there are no experimental studies for describing the characteristics of atmospheric boundary layer in the centre of Baghdad city, except the meteorological data recorded most of the time in

weather station locating outside of the center. Of course, mean wind speed values in urban sites largely reduce from those of in rural sites. In such cases there is a need for the diagnosis of the mean wind speed with height. This needs to be computed by extrapolating data upward at the measurement site.

Under neutral and non-neutral conditions, the variation of wind speed with height is well described by the logarithmic or the power laws (for more details, see references [1] and [2]). Many authors and workers described wind profiles over different terrains, for example, Carl et al. [3] showed the wind and temperature profiles from towers over homogeneous terrain using logarithmic relationship. Holtslag [4] analyzed the wind profile observed at the 213 m tower at Cabauw, the Netherlands. Using numerous large-eddy simulations, Brown et al. [5] investigated the behavior of wind profile in unstable boundary layer and found that for steady cases the effect of entrainment has little impact on the wind profile at lower levels, expect for cases with very strong baroclinicity. Beyond the surface layer, an extension to Monin-Obukhov (M-O) theory to predict the behaviour of the wind profile have been formulated for the entire boundary layer over land and sea surfaces (for more details, see references [6] and [7] respectively). A comparison among reconstructed vertical profiles of wind derived by analytical, iterative and simple power law methods has been presented by Musson-Genon [8]. Lastly, Al-Jiboori [9] studied wind structures over the urban centers using a simple power-law expression.

In the above references, logarithmic and power relations have been found to satisfy observations in the lower atmosphere up to at least 200 m. These profiles were found to be functions of both roughness length and stability factor. Thus, in this research work, I attempt to predict and diagnosis the wind profiles over Baghdad city using logarithmic and power laws based on the data measured at some heights above the ground located among the roughness elements, meadows and trees. Also drag coefficient related to rough surfaces is also calculated at these heights and then is studied its variation with atmospheric stability.

2. The frame of analysis

The distribution of wind speed with height can be obtained in the lower atmosphere using two common laws: classical logarithm and

empirical exponent power. In general, wind velocity at any height as will be shown in section 3 depends upon the roughness parameters, e.g. surface roughness (Z_0) and zero-plane displacement lengths (Z_d), friction velocity (U_*) and the atmospheric stability. Unfortunately, as will be illustrated in next section, there is a few data under stable conditions, thus, the expressions concerning with near neutral and unstable conditions will present in this paper.

2.1 Logarithmic wind law

The wind speed, U , at any height, Z , above the ground in the surface boundary layer can be derived by [1, 2]:

$$U(Z) = \frac{U_*}{\kappa} \left[\ln \frac{Z - Z_d}{z_0} - \Psi_m \left(\frac{Z}{L} \right) \right] \quad (1)$$

where U_* is the friction velocity, κ the von Kármán (taken as 0.4 in this paper [1, 2]) and $\Psi_m(Z/L)$ is an empirical function that describes the stability correction given below for the stability with L is the Monin-Obukhov length ($= -U_*^3 \bar{T} / kg \overline{w'T'}$, here \bar{T} is mean temperature, g the acceleration of gravity and $\overline{w'T'}$ the turbulent heat flux).

$$\Psi_m(\xi) = \int_0^\xi \frac{1 - \Phi_m(\xi)}{\xi} d\xi \quad (2)$$

where $\xi = Z/L$ and Φ_m is the dimensionless function of wind gradient which is a function only of Z/L given as

$$\Phi_m \left(\frac{Z}{L} \right) = \frac{\kappa Z}{U_*} \frac{\partial U}{\partial Z} \quad (3)$$

In this paper, the stability parameter will be indicated by Richardson number, Ri , given as

$$Ri = \frac{g}{\bar{T}} \frac{\Delta T / \Delta Z}{(\Delta U / \Delta Z)^2} \quad (4)$$

According to M-O similarity theory for the surface layer, Ri should be a function of Z/L and in unstable air becomes

$$Ri = Z/L \quad (5)$$

which is verified using the Kansas data [10]. For practical purpose, empirical form has been widely used to describe the relation between Φ_m and Z/L in unstable air

$$\Phi_m \left(\frac{Z}{L} \right) = \left(1 - \gamma \frac{Z}{L} \right)^{-1/4} \quad (6)$$

where γ is a constant based on the observational data, which ranges from the value of 15 [10] to 16 [3] for most experimental studies, so the mean value of 15.5 is taken in this paper.

In neutral condition (when $Z/L \rightarrow 0$), when heat convection is negligible and the lapse rate is near adiabatic. This condition will generally be satisfied with very strong winds. We must have $\Phi_m(0) = 1$ and $\Psi_m(Z/L) = 0$, Eq. (1) reduce to

$$U(Z) = \frac{U_*}{k} \ln \frac{Z - Z_d}{Z_o} \quad (7)$$

But in unstable air when convection is dominant comparing to mechanical turbulence, the expression for Φ_m becomes

$$\Psi_m\left(\frac{Z}{L}\right) = 2 \ln\left(\frac{1+x}{2}\right) + \ln\left(\frac{1+x^2}{2}\right) - 2 \tan^{-1} x + \frac{\pi}{2} \quad (8)$$

where $x = (1 - \gamma z/L)^{1/4} = \Phi_m^{-1}$.

In some recent studies concerning with the formulation of wind profile for the surface layer [8], entire [6] and marine [7] PBL for a homogeneous flows (e.g., over flat or open sea surfaces) and stationary conditions, U_* has been considered constant with surface-layer height. But in non-homogeneous flows (e.g., over urban or wood areas), the situation is different whereas Louka et al. [11] found that U_* increases with the height from very small values at the lower part of roughness sublayer towards a virtually constant value. Thus, the variation of U_* with height must be taken into account.

2.2 Power-exponent law

Engineers have generally preferred to estimate wind speed at higher heights (Z_2) by the use of the common power law [1]

$$U_2 = U_1 \left(\frac{Z_2 - Z_d}{Z_1 - Z_d} \right)^p \quad (9)$$

where U_1 is the mean speed at a reference height, $Z_1 - Z_d$. Although Eq. (9) does not have a sound theoretical basis, it provides a reasonable fit to the observed wind profile over a small height range in the lower part of PBL. Since wind ratios are affected by heat convection, thus the exponent p depends on both surface roughness and atmospheric stability. To demonstrate this effect and dependence, rearrange Eq. (9) with assuming that $U_2/U_1 = U$ and $Z_2 - Z_d / Z_1 - Z_d = Z$

$$p = \frac{d \ln U}{d \ln Z}$$

differentiate it with respect to height Z ,

$$p = \frac{Z}{U} \frac{dU}{dZ}$$

Combining (3) and (1) with the above equation, we obtain

$$p = \frac{\Phi_m\left(\frac{Z}{L}\right)}{\ln \frac{Z - Z_d}{Z_o} - \Psi_m\left(\frac{Z}{L}\right)} \quad (10)$$

It is obvious from (10) that p increases with the increase roughness and decreases with the instability.

3. The Site and data

To calculate wind speed at higher heights through the lower part of PBL, the data such as wind speed, its direction and temperature made over the called Bab Al-Mhadham located at the centre of Baghdad city ($32^\circ 14''$ N, $44^\circ 14''$ E and 31.7 m above mean sea level) are used. These data were measured by two sets of classical slow-response instruments such as three-cup anemometer, wind vane and thermometer. These instruments were mounted on two masts with heights 15 and 20 m which were set up on one of the roofs belonging to the engineering college buildings. In briefly, the field around the measurement area consists of mostly government offices with different heights including very big public hospital, scientific institutes, ministries, public schools and so on. Many low houses with 4 m height are located to the east of measurement mast. Lastly many old and tall trees are scattered in whole area around the mast. A full description of Bab Al-Mhadham facilities can be found in [12]. They have been calculated the Z_0 and Z_d using the logarithmic wind profile equation from the data under neutral conditions according to wind direction. The values of Z_0 and Z_d (m) range from 0.7 to 1.7 with average 1.2 and from 4 to 17.9 with mean value of 7.5, respectively.

The data used at each level were observed at the same time at afternoon from 4:00 to 7:00 local standard time for the period from 4 to 20 April 2006. These data were recorded every minute for interval of 20 min, and then twenty-minute averages were computed. The atmospheric stability in terms of Richardson number was determined using Eq. (4). More than 50 runs were obtained with 28 runs in neutral and near neutral conditions ($-0.01 < Ri < 0.01$) and remaining runs were mostly in unstable conditions and a few runs in stable conditions.

4. Results and discussion

4.1 Friction velocity

In urban environments with high roughness, i.e. mostly non-homogeneity surfaces, the

momentum flux based on friction velocity ($=\rho U_*^2$) is not constant in the surface layer. In other speech, U_* can reflect the rough status of a surface. This result has been found in many studies conducted to study turbulent characteristics of urban atmosphere (e.g., [13] and [11]). In order to recalculate wind speed at the two levels by use of logarithmic equation, it is required to determine first U_* . According to the values of Ri calculated by (4), the stability function $\chi_m(Ri)$ was calculated from (8) using $\gamma=15.5$ for unstable air, and then used to obtain U_* by rearrangement Eq. (1) for all speed wind measurements. The U_* results are plotted against atmospheric stability in Figure 1.

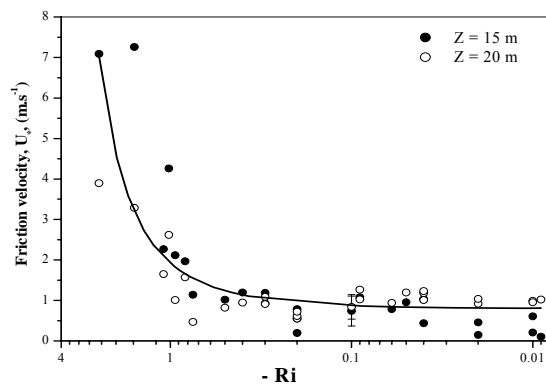


Figure 1: Friction velocity derived at two heights 15 and 20 m versus atmospheric stability.

In near neutral conditions, U_* values are approximately constant around 0.8 m.s^{-1} with significant scatter which is expected because surface roughness features around the experimental site are largely changed. It can also be illustrated that U_* values at level 15 m are smaller than those at 20-m level. Although the small difference between the two measurement level (which is 5 m), the reason of the differences in U_* at two levels is to a skimming flow effect as well as roughness element effect on the wind flow as shown in [11] and [13]. The linear increase in the values of U_* over unstable conditions, $-Ri < 0.7$, is obvious as shown in Figure 1. The large U_* values in this figure are not surprising because they have a relatively response to the changing in the height and generally increase with rough surfaces ([14] and [15]). However, through the data points the fitting curve is drawn by the solid line which follows the expression

$$U_* = 0.8 \text{EXP}(-R_i/1.14) \quad (11)$$

4.2 Drag coefficient

The reflection of rough surfaces can be deduced by drag coefficient, C_D , which is required for many practical purposes, e.g. to relate momentum flux to the mean wind profile and the parameterization of the surface shearing stress in numerical models. Integration of (3) with respect to height results the following expression for C_D at any height and stratification:

$$C_D(Z) = \left(\frac{U_*}{U}\right)^2 = \frac{k^2}{\left(\ln \frac{Z-Z_d}{Z_o} - \Psi_m(Z/L)\right)^2} \quad (12)$$

Thus, C_D is a function of height, roughness length and stability. For neutral stability, $Z/L \rightarrow 0$, C_D becomes function of Z_o and Z , i.e. C_D is proportional to Z and Z_o , as

$$C_{DN}(Z) = \frac{k^2}{\left(\ln \frac{Z-Z_d}{Z_o}\right)^2} \quad (13)$$

Note that for a given height and wind speed, C_D increases with increasing surface roughness. Also at any reasonable wind speed for a particular surface, C_D will be deemed to be the constant value corresponding to that surface.

However, from the values of U_* and U , C_D values were calculated from (12) at each level for all stabilities and presented in Fig. 2, in which the dependence of C_D on both the measurement height and stability is fairly clear. The greater C_D -values at 20 m level are more fair comparing to those at another level over all stabilities. Over near neutral regime, the C_{DN} results have constant behavior with values of 0.048 and 0.029 for two heights 15 and 20 m, respectively. These observational results are in consistent well with theoretical prediction of (13) when using the values of \bar{Z}_o and \bar{Z}_d mentioned in section 3. Under unstable conditions, C_D values for both heights logarithmically increase with increasing in instabilities.

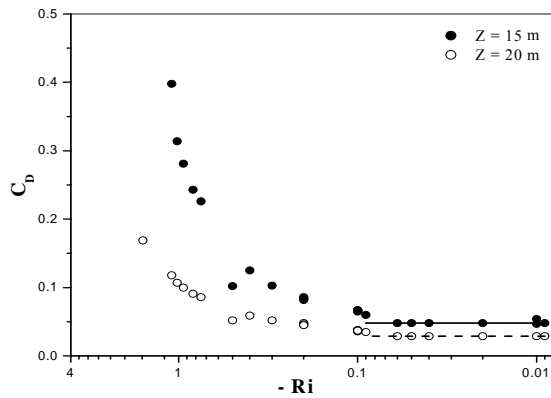


Figure 2: Same as Fig. 1, but for drag coefficient. Solid and dashed lines represent its averages at 15 and 20 m over neutral regime, respectively.

The dependence of C_{DN} on the wind speed can also be observed in neutral air when plotting C_{DN} results for each level against their corresponding values of wind speed as illustrated in Figure 3. It is interesting to see that the C_{DN} data points for $0.7 < U_{15} < 4.7$ ($m.s^{-1}$) at height 15 m not also separate clearly from those for $2.5 < U_{20} < 7.5$ ($m.s^{-1}$) at 20 m, but also are larger than those at 20 m. However C_{DN} results exponentially decrease with increasing wind speed. The solid line is fitted well the C_{DN} data against wind, which is expressed as

$$C_{DN} = 0.018 + 0.064 \text{EXP}(-U/4.86) \quad (14)$$

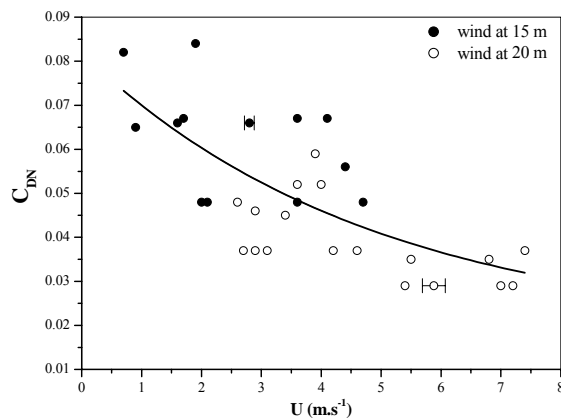


Figure 3: Neutral drag coefficient at the two heights 15 and 20 m as function of wind speed.

4.3 Wind profiles

In this section, wind speed profiles will be simulated by use of two laws (1) and (9) as a function of atmospheric stability parameter such as near neutral and unstable stratification. The construction and the outline of wind profile simulated by each law are presented in the next two subsections and then their comparison with each other will be discussed too.

4.3.1 Logarithmic wind profile

According to the discussions in subsection 4.1, it is more interesting to simulate the vertical profile of wind with making a simple modification for Eq. (1). This can be done by substitute empirical relation for U_* (Eq. 11) in Eq. (1):

$$U(Z) = \frac{0.8 \text{EXP}(-R_i/1.14)}{k} \left[\ln \frac{Z - Z_d}{Z_0} - \Psi(R_i) \right] \quad (15)$$

Before extrapolating the wind at any height above the ground, Eq. (1) has been examined using the wind observations for the two heights 15 and 20 m. Using \bar{Z}_0 , \bar{Z}_d as well as U_* and Ψ_m given by (8) for certain R_i , wind speeds at these heights have recalculated by (1). After this, values of estimated 15 and 20 m wind speed $(U_{15 \text{ est}})_L$ and $(U_{20 \text{ est}})_L$ are compared to the experimental observations taken in this paper for each height ($U_{15 \text{ obs}}$) and ($U_{20 \text{ obs}}$) by plotting them in Figures. 4a and 4b, respectively. Furthermore, in order to know the extent of variation between the observed and measured wind speed, the correlation coefficients (R) and standard deviation (SD) were calculated.

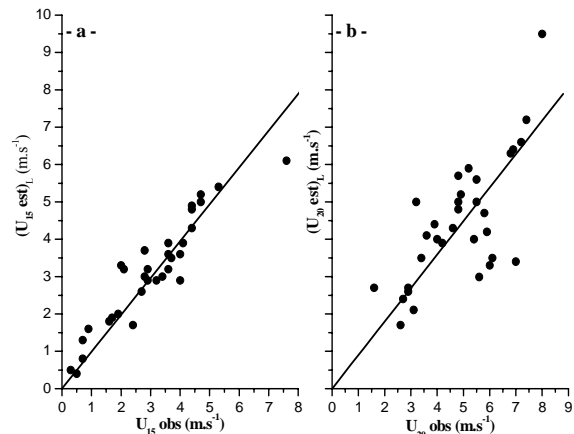


Figure 4: Comparison of observed U values with estimated U values by Eq. (15) at (a) 15 m and (b) at 20 m.

In Figure 4a, at level 15 m there is a very good agreement between $(U_{15 \text{ est}})_L$ and $U_{15 \text{ obs}}$ values with low scatter. Thus, the linear expression between them is given as $[(U_{15 \text{ est}})_L = 0.99 U_{15 \text{ obs}}]$ and is drawn in the figure by solid line. This agreement is also evident from the values of R ($= 0.93$) and SD ($= 0.57$). Meanwhile the relatively good agreement at the 20 m level is shown in Fig. 4b with large scatter. The best fitting between the data points of $(U_{20 \text{ est}})_L$ and $U_{20 \text{ obs}}$ can be given by the linear relation $[(U_{20 \text{ est}})_L = 0.9 U_{20 \text{ obs}}]$ represented by solid line. Their values have lower R and larger SD which are 0.72 and 1.2, respectively. Although the

small difference between the two measurement heights (which is 5 m), measured wind speed values at 20 m height are relatively larger than those at 15 m. Alternatively, the differences between the values of $(U_{20} \text{ est})_L$ and $U_{20} \text{ obs}$ are expected because the $(U_{20} \text{ est})_L$ values are slightly increased especially in neutral air. This increase, certainly, will lead to large scatter between them.

The more interesting in this paper is to show how the slightly wind speed gradient vary with height according to stability parameter. This can be performed when plotting the observed wind speed in x-axis opposite $\ln(Z-Z_d/Z_0) - \Psi_m(Ri)$ in ordinate axis as seen in (Fig. 5), in which two and three classes of near neutral and instability cases are displayed, respectively. For each data point on the graph, the horizontal lines represent the standard deviations of wind data. It can be seen that the vertical gradient of wind (slope of vertical lines represented by U_*/κ) is largest in neutral air and progressively decrease to be small upwards in unstable air. This variation in the slopes for the vertical lines can be provided a signal to the dependence of U_* on the height and stability.

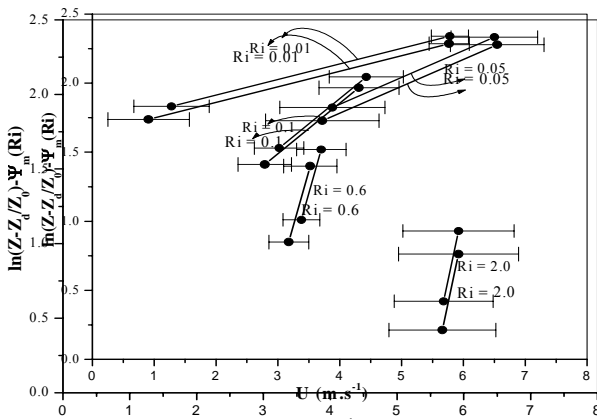


Figure 5: Variation of $\ln(Z-Z_d/Z_0) - \Psi_m(Ri)$ as function of wind speed under different intensities of instability.

The simulated profiles of wind are derived for each 20 m up to less than 100 m. The latter height is chosen because the logarithmic relation during adiabatic (neutral) conditions has been found to satisfy observations in the lower atmosphere up to 100 m as reported in [6, 16]. The wind profile expected through the depth of 100 m is presented in Figs. 6a and 6b according to stability such as for near neutral conditions ($Ri=-0.03$) and for unstable conditions ($Ri=-3$), respectively. In neutral air the wind is largely

increased with height while it becomes slightly increased in unstable air.

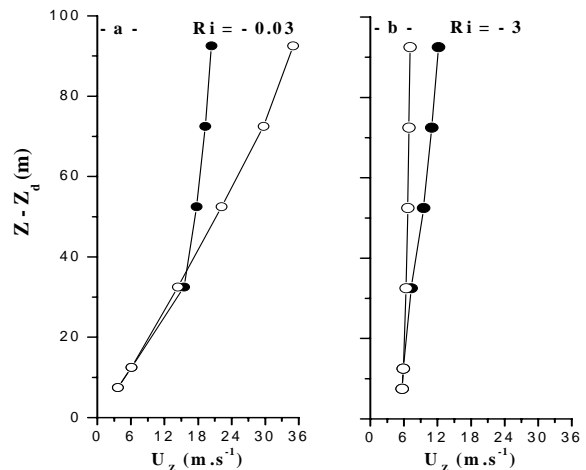


Figure 6: Simulated vertical profiles of wind speed calculated by (15) and (9) for (a) near neutral and (b) unstable conditions.

4.3.2 Power-exponent law

Employing the observational data for winds at the two levels, the exponent p is calculated for all runs in this work, and then, their values are taken as averages in accord with stability. Mean p -values are 0.97 ± 0.4 for neutral air and 0.09 ± 0.4 for unstable air in this work. It should be noted that the p -value decreases when increasing instability whereas convection has important role in reducing power exponent [2]. The large value of $p=0.97$ is not surprising because it is found to be dependent not only on stability but also on the surface roughness parameters, Z_0 and Z_d . The approximate value (≈ 0.95) can also be obtained from the expression below when Z_d is not small (for more details, see reference [1]).

$$p = \frac{Z}{(Z - Z_d) \ln\left(\frac{Z - Z_d}{Z_0}\right)} \tag{15}$$

With the above values of p for both neutral and unstable conditions, the wind profile was also calculated for the same 100 m height used in the previous subsection. Through this height range the exponent was to be constant with height as pointed out by [1].

The power-exponent law can provide good results about the shape of wind profile over a certain area whereas it is used to give a reasonable fit to the observed wind profiles in the lower part of ABL as shown in [2, 8]. Before calculating wind profile by power law, which was tested by estimating wind speed at height 20 m, $(U_{20} \text{ est})_p$, using the values of p derived and

wind observations at height 15 m in this paper. The results of $(U_{20} \text{ est})_p$ against those observed $U_{20} \text{ obs}$ are presented in (Fig. 7), in which $(U_{20} \text{ est})_p$ results are in good agreement with those observed at 20 m with less scattering (where $R=0.88$ and $SD=0.99$) comparing to the results obtained in Fig. 4b. The solid line drawn through the data points gives the reasonable fit, which follows the relation $[(U_{20} \text{ est})_p=0.97 U_{20} \text{ obs}]$. Therefore, power law can provide good results for wind speeds, and hence can be employed to derive the vertical profile of wind. With derived p values in this study under near neutral and unstable conditions the wind speed at every 20 m were calculated up to 100 m. They were, then, plotted versus the height as shown in Figures 6a and 6b, respectively. The shape of the profile for the neutral air (Figure 6a) has high gradient with height comparing to that for unstable air (Figure 6b).

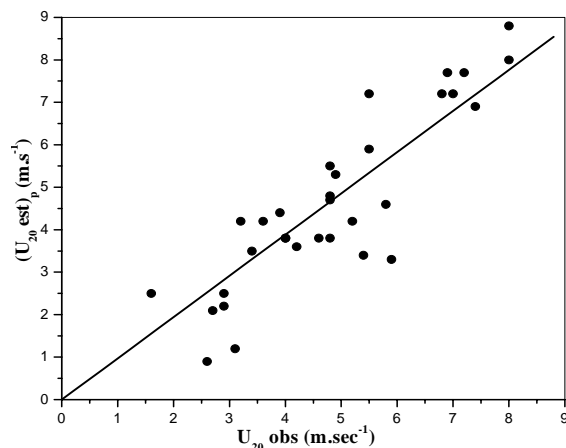


Figure 7: Comparisons of observed U values with those estimated by Eq. (9) at 20 m height.

4.3.3 Comparison between two laws

As discussed in previous subsections, both logarithmic and power laws are dependent upon the surface roughness and atmospheric stability, but in different mathematical forms as shown in (1) and (9). Logarithmic equation (1) do not need to wind data at a reference height for calculating wind at the next height but the need to Z_0 , U^* and z_m (Ri) for nonadiabatic conditions. This equation could be active at heights adjacent to the edge of the roofs of roughness elements, thus it is incorrect in practical applications especially for the heights far away from the surface layer as shown in Fig. 6 because wind flow do not affected by friction force and hence geostrophic wind will be balanced by the pressure gradient and gravity forces.

Power exponent in (9) implies surface roughness and stability effects and thus predicated wind by it at any height has to require at a reference height. Therefore, this law could often be offered correct data for a certain height range especially at adjacent heights to the reference. Trough 325 m meteorological tower set up in Beijing city, Al-Jiboori [9] found that the empirical value of exponent ($p = 5.2$) was approximately constant for near neutral conditions.

(Figures 6a and 6b) show the predicted vertical profiles of mean wind in neutral and unstable air using logarithmic ($-●-$) and power exponent ($-○-$) relationships. In near neutral air ($Ri = -0.03$) the wind values derived by two laws (1) and (9) are very close to each other for two heights of 30 and 50 m and hence the differences between their results gradually start from 70 m up to 100 m. The same result is also found in unstable air, but a significant difference grows. After 100 m height, the vertical profile of wind over any site and for any stability will be, of course, far away and overestimated from the logical results. It should be noted that for neutral conditions the variation of wind with height is more logarithmically increased than in unstable conditions, in which profile derived by logarithmic law is assumed to be in the form of steep gradient (just like derived by power law) but it fairly increases with height in logarithmic form.

5. Conclusions

This paper has attempted to estimate the vertical profiles of wind speed in near neutral and unstable stratification over Baghdad city. These wind profiles were derived from logarithmic and power-exponent laws up to 100 m. Before deriving wind speed vertically, the valid of estimated values by those laws at 20 m height was compared to these observed in this paper and the result was in good agreement. The used data of wind and temperature in this paper were measured at two levels 15 and 20 m by three-cup anemometer and thermometer, respectively. The atmospheric stability parameter is indicated by calculating the Richardson number. The main results can summarize as:

1. The constancy in U^* values which are around 0.8 m.s^{-1} is obvious over near neutral conditions and then they exponentially increase when $-Ri < 0.7$.

2. Within urban canopy U_* values are small at lower levels and then gradually increase upwards up to be constant above the roughness elements.
3. The dependence of C_D on height and stability is clear, whereas in neutral air $C_D=0.048$ at 15 m and $=0.029$ at 20 m, while in unstable air their values are increased when $-Ri < 0.2$.
4. In near neutral air, the results for C_{DN} were found to decrease with strong wind speed.
5. Wind speed values calculated from logarithmic law at 20 m are slightly larger than these observed at the same height.
6. While calculated values at 20 m by exponent law are in good agreement with those observed.
7. Based on wind speed at the two heights the exponent p was calculated by use of rearrangement power law. The results of p were 0.97 and 0.09 in near neutral and unstable air, respectively.
8. Wind speed profile derived by power law gives a reasonable result rather than the logarithmic law under unstable conditions, while the result is inversed for neutral conditions.
5. Brown A.R.; Beljaars A. C. and Hersbach H. **2006**. Errors in parameterizations of convective boundary layer turbulent momentum mixing, *Quartly Journal of Royal Meteorological Society*, **132**:1859-1876.
6. Gryning, S-E.; Batchvarova E.; Brümmner, J. rgensen, H. and Larsen S. **2007**. On the extension of the wind profile over homogeneous terrain beyond the surface layer, *Boundary-Layer Meteorology*, **124**:251-268.
7. Peñ a A.; Gryning, S-E and Hasager, C. B. **2008**. Measurement and modeling of the wind speed profile in the marine atmospheric boundary layer, *Boundary-Layer Meteorology*, **129**: 479-495.
8. Musson-Genon, L.; Dupont E. and Wendum D. **2007**. Reconstruction of the surface-layer vertical structure from measurements of wind, temperature and humidity at two levels, *Boundary-Layer Meteorology*, **124**: 235-250.
9. Al-Jiboori, M. H. **2003**. Roughness and turbulence characteristics in urban Beijing city, Report for post-doctorate research, Chinese academy of sciences, Institute of atmospheric physics. pp.64.
10. Businger, J. A.; Wyngaard, J. C.; Izumi, Y. and Bradley, E. F. **1971**. Flux-profile relationships in the atmospheric surface layer, *Journal of Atmospheric Sciences*, **28**:181-189.
11. Lucka, P.; Belcher, S. E. and Harrison, R. G. **2000**. Coupling between airflow in street and the well-developed boundary layer aloft, *Atmospheric Environment*, **34**:2613-2621.
12. Al-Jiboori, M. H. and Al-Daraji A. G. **2010**. Aerodynamic surface roughness of Baghdad derived from wind observation, *Journal of Al-Nahrain University*, **13**(1):86-92.
13. Högstörm, U.; Bergtrm, H. and alexnaderrson, H. **1982**. Turbulence characteristics in a near neutrally stratified urban atmosphere, *Boundary - Layer Meteorology*, **23**: 449-472.
14. McIntosh D. H. and Thom, A. S. **1981**. *Essentials of Meteorology*. Taylor and Francis, London, pp. 59.
15. Garratt, J. R. **1992**. *The Atmospheric Boundary Layer*. Cambridge University Press, Cambridge, pp.316.
16. Lumley, J. L. and Panofsky, H. A. **1964**. *The Structure of Atmospheric Turbulence*. Intersciences, London, pp.239.

Acknowledgement

I am grateful to Prof. Sven-Erik Gryning from Wind Energy Department, Risø National Laboratory for Sustainable Energy, Technical University of Denmark, for his help in sending me some recent papers.

References

1. Panofsky, H. A. and Dutton, J. A. **1984**. *Atmospheric Turbulence: Models and Methods for Engineering Applications*. Wiley-Intersciences, John Wiley and Sons, New York, pp.397.
2. Arya, S. P. **2001**. *Introduction to Micrometeorology*, 2nd editions, Academic press, A Harcourt Sciences and Technology Company, San Diego, USA, pp.420.
3. Carl, D. M.; Tarbell, T. C. and Panofsky, H. A. **1973**. Profiles of wind and temperature from towers over homogeneous terrain, *Journal of Atmospheric Sciences*, **30**:788-794.
4. Holtslag, A. A. **1984**. Estimates of diabatic wind speed profiles from near-surface weather observations, *Boundary-Layer Meteorology*, **29**:225-250.

